FAST EVOLUTION OF BACTERIA IN THE PRESENCE OF ANTIBIOTIC GRADIENTS

Krisztina Nagy

OTKA PD 124889
Final report
01.10.2017-31.08.2021.

Spatiotemporal structures and heterogeneities are common in natural habitats, yet their role in the evolution of bacterial resistance and other basic ecological phenomena is still to be uncovered. My research focused on better understanding the role of the microenvironment (chemical and physical heterogeneities) in the life of microbial communities with a special interest on the evolution of resistance. For this purpose, we combined modern methods of microfluidics, molecular biology techniques and classical microbiology methods.

1. Escherichia coli in spatial gradients of antibiotics

The driving force behind the research on antimicrobial resistance is twofold. On the one hand, it is an important topic in basic research that helps to answer fundamental questions about evolution. On the other hand, bacteria with antibiotic resistance pose a significant threat to human health, and through that to society. During the grant period the main biological problem we were focusing was to study the effect of chemical concentration gradients of antibiotics on the evolution of bacterial resistance.

Chemical gradients are widespread in natural habitats (including the human body), in which gradient-dependent phenomena like chemotaxis might occur. Microfluidic technologies provide the tools to establish and control habitat gradients in space and time to effectively explore their role in evolutionary processes.

The concentration-dependent effects of antibiotics suggest that uneven distribution of antimicrobial agents may substantially impact the evolution of resistance. Some theoretical studies indicate that such heterogeneous distribution, especially linear concentration gradients of these chemicals, might accelerate the evolution of resistance. In the past decade, a handful of studies appeared in the literature to explore the evolution or resistance in the presence of antibiotic gradients, which yielded seemingly contradicting results. Therefore, we aimed to perform a systematic set of experiments to explore the effect of antibiotic concentration gradients.

We used a home-made microfluidic gradient generator device to perform these experiments (Figure 1A,B). It consists of two large reservoirs and a narrow observation channel that are separated with a porous membrane. Each side of the observation channel overlaps with the reservoirs in a narrow region. Diffusion of molecules from one reservoir to the other through the membrane establishes a linear concentration gradient across the 1.2 mm width of the channel, where cells are injected (Figure 1C). The slope of the gradient might be changed by applying different concentrations of antibiotics in the reservoir.

In the beginning of the project I cultured our wild type *E. coli* strain in different media. We expected that nutrient supply and growth rate/division time has an effect on the evolutionary processes. I chose the nutrient rich LB medium, and M9 supplemented with glucose and/or casamino acids to work with in the first microfludic experiments. It turned out after a couple of experiments that LB provides a better condition to perform the planned evolution experiments, since in case of the minimal media I did not observed the appearance of insensitive bacterial populations within a reasonable timeframe. This observation also gives us the valuable information on the importance of resource supply under such circumstances. Of course, it would be interesting to see how long would it take to reach resistance and what circumstances are needed, under nutrient poor conditions (if it is possible at all), however, due to the limited time and the long timeframe of these evolution studies, most of my results are coming from experiments carried out using LB medium.

1.1 Emergence of resistant *E. coli* mutants in microfluidic on chip antibiotic gradients

Evolution of resistance in ciprofloxacin gradients

We tested the effect of the growth inhibitor ciprofloxacin on fluorescently labeled *E. coli* cells. The target of this antibiotic is the gyrase enzyme which is necessary during cell division. The maximum concentration of ciprofloxacin within the device was always above the minimal inhibitory concentration (MIC) measured on the wild type cell culture. We used different concentrations of ciprofloxacin (3-6× MIC) for gradient formation and performed experiments for 1-3 days. We observed the emergence of a fast-growing insensitive population within 24 hours on the low (sublethal) antibiotic concentration side of the observation channel. These cell assemblages usually showed high fluorescence and behaved like biofilms propagating towards the high (lethal) concentrations (Figure 1D-F). In some cases we observed the emergence of localized subpopulations (often with altered fluorescence intensity) with considerable growth advantage (Figure 2B).

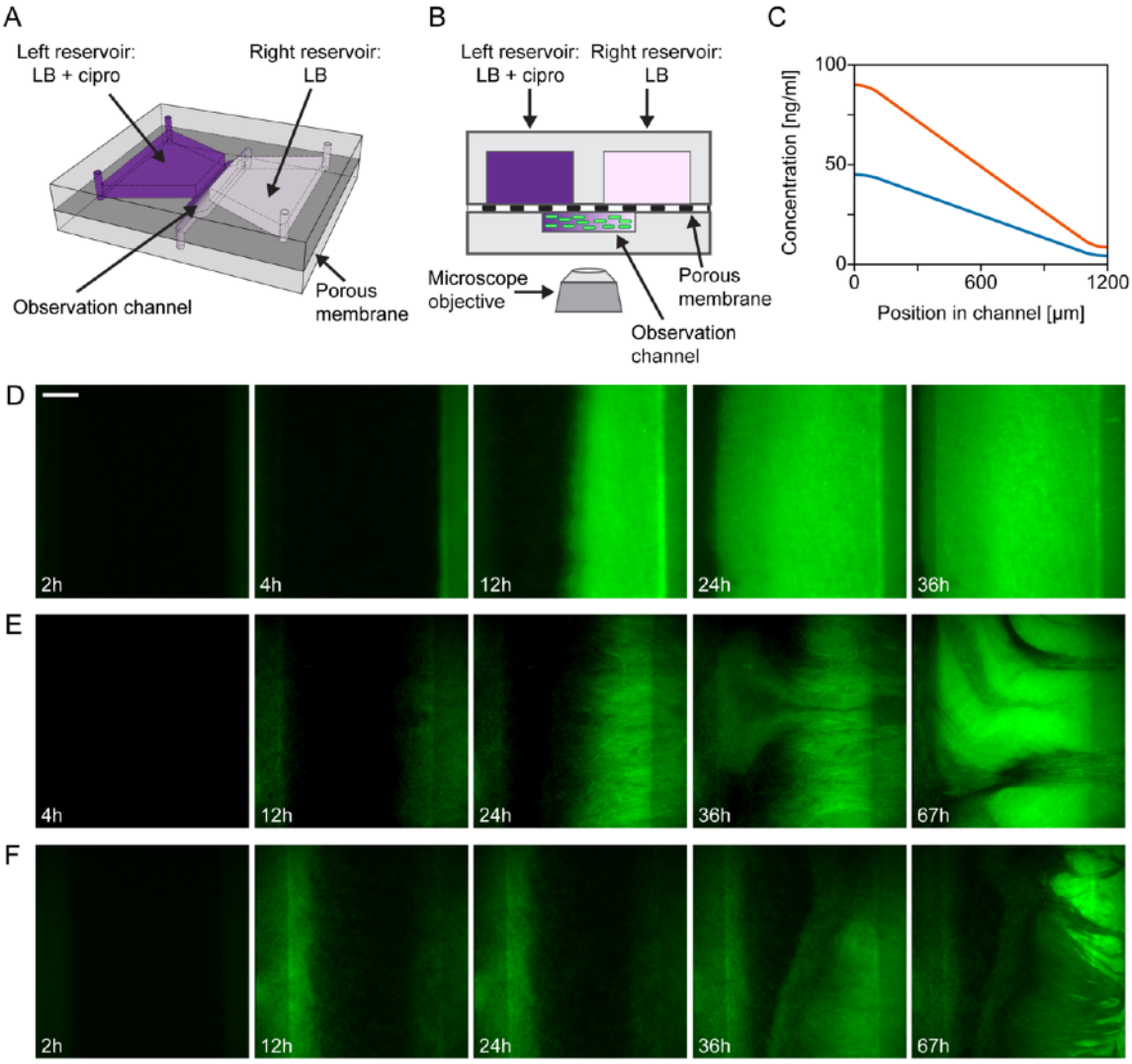

Figure 1. Outline of the gradient generator microfluidic setup and time-lapse images of growing bacterial populations within. (A) *Schematic drawing of the device (not-to-scale).* ***(B)*** *Cross-sectional view of the device (not-to-scale).* ***(C)*** *Theoretical profiles of ciprofloxacin concentration across the width of the observation channel in case of loading 48 ng/ml (3× MIC, blue curve) or 96 ng/ml (6× MIC, orange curve) antibiotic solution into the left reservoir.* ***(D–F)*** *Fluorescent images showing the distribution of bacteria across the observation channel (scale bar is 200 µm). Maximum ciprofloxacin concentrations (left side) are as follows:* ***(D)*** *3× MIC;* ***(E)*** *3× MIC; and* ***(F)*** *6× MIC*

In case we started the experiment with a low cell number (~1,000 cells) and gained high magnification microscopy images, we could study the morphology of the cells within the device. Beside the filamentous bacteria (which form upon ciprofloxacin treatment even at sublethal

concentrations), we detected normal sized, rod-shaped bacteria as well (Figure 2C,D). Although the filamentous cells showed less surface attachment and mobility, they formed a dense interwined multicellular mass that maintained some spatial structure.

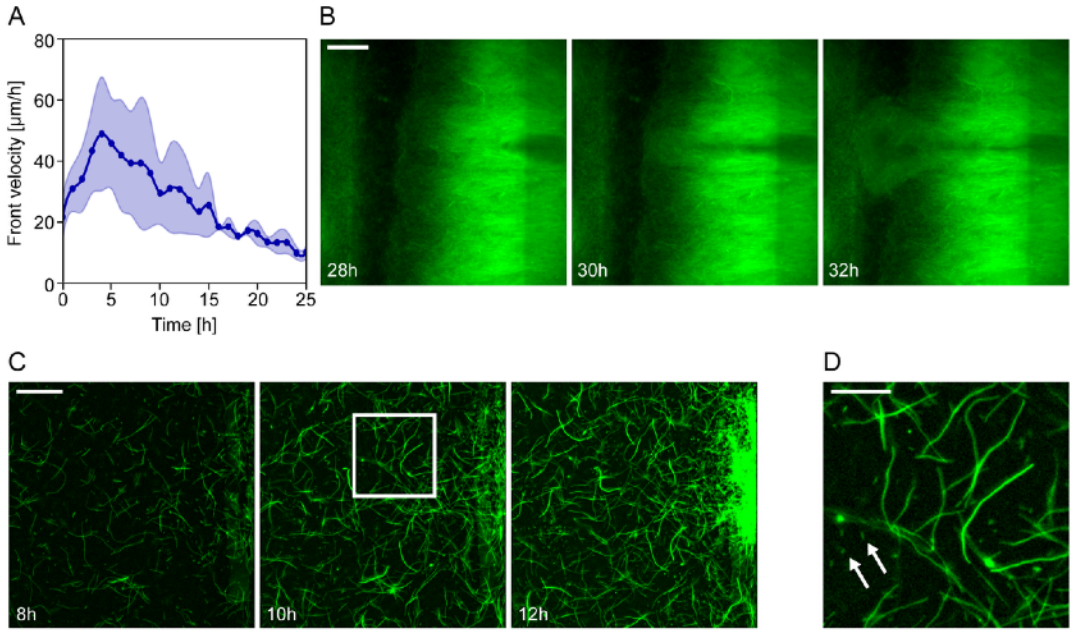

Figure 2. Formation and expansion of resistant E. coli populations in ciprofloxacin gradients. (A) *Changes in the velocity of the propagating front in time. The graph represents the average of the front velocity in experiments with 3× MIC gradient (thick line, n = 4) together with the standard deviation. Zero time marks the moment the intense expansion of the population starts.* ***(B)*** *Fluorescence images showing the emergence of a less bright but fast-growing subpopulation at a specific location on the low ciprofloxacin side of the channel (scale bar is 200 µm).* ***(C)*** *Emergence and growth of a resistant subpopulation on the low antibiotic concentration side of the observation channel. Series of fluorescence images taken at different time points of the experiment (scale bar is 50 µm).* ***(D)*** *Zoom-in of the image taken at 10 h to show E. coli cells with different morphologies (scale bar is 20 µm). Arrows indicate some normal size rod-shaped cells among filamentous ones.*

To investigate further what changes occur in bacteria that experience the microfluidic environment and the ciprofloxacin gradient, cells were extracted form 13 devices for MIC measurements and whole genome sequencing studies. Altogether 105 colonies were used for MIC measurements and 23 of them were sequenced. To our surprise, we learned that experiencing the microfluidic environment itself conferred bacterial cells a slightly increased value of MIC even when not exposed to the antibiotics *on-chip*. Furthermore, results show that MIC change correlates with the duration of exposure to the antibiotic gradient. Samples extracted after 48 h typically exhibit 2-4× MIC change, while a 1-30× change was measured for samples collected after 72 h. Measured MIC values varied even within samples taken from a single experiment, which demonstrates a compound community development in the microfluidic habitat, giving rise to genetic diversity.

Whole genome sequencing data suggest that high level of resistance (above 20× MIC) is associated with single nucleotide point mutations in *gyrA* which is the target of ciprofloxacin. Lower level of resistance is reached by alterations in genes associated with the assembly of the outer membrane (*rfaG*, *rfaQ*, *ompF*, *dsbA*) or genes related to efflux activity (*marR*, *soxR*).

In conclusion, our experiments suggest that surface associated biofilm formation is necessary for the observed evolution in the presence of ciprofloxacin gradient. In the absence of an explicit structure of the habitat, this multicellular formation led to a spatial structure of the population with local competition and limited migration. Therefore, such structures can function as amplifiers of selection and aid the spread of beneficial mutations. We found that the physical environment itself induces stress- related mutations that later prove beneficial when cells are exposed to antibiotics. This shift in function suggests that exaptation occurs in such experimental scenarios. The above two processes pave the way for the subsequent emergence of highly resistant specific mutations. These results have been published in Frontiers in Microbiology [5].

Evolution of resistance in ampicillin gradients

In the research project I was planning to study the effect of chemical concentration gradients of antibiotics with different modes of action. The second antibiotic I started to work with was the cell wall synthesis inhibitor ampicillin. Both ampicillin and ciprofloxacin are bactericide antibiotics with clinical relevance.

I performed the same set of experiments as described above. I used the same gradient generator microfluidic device, however, I put ampicillin in one of the reservoirs (always left side in the images). As a maximum concentration, I applied 3× or 6× MIC ampicillin solution. The response of bacteria was very similar in the presence of ampicillin gradients as I observed in case of ciprofloxacin. An insensitive bacterial population emerged on the sublethal antibiotic concentration side of the observation channel that later colonized other parts of the habitat (moved forward to the high antibiotic concentration regions). Time-lapse fluorescence microscopy image series presented in Figure 3. are taken from characteristic experiments. We observed the formation of localized subpopulations in ciprofloxacin gradients, however, in case of ampicillin these locii are even more enhanced. Figure 3C shows a zoom-in into an area of the low ampicillin concentration side of the observation channel from where cells start to grow intensively. The typical morphology of these cells is elongated, filamentous-like. The observed subpopulations, in the right side of the channel, merge and colonize the habitat. Mutants with lower or higher fluorescence intensity can emerge over time (Figure 3A). Based on our experiments so far, it seems that surface associated biofilm formation is important in the early phase of the evolution of resistance in ampcillin gradients as well.

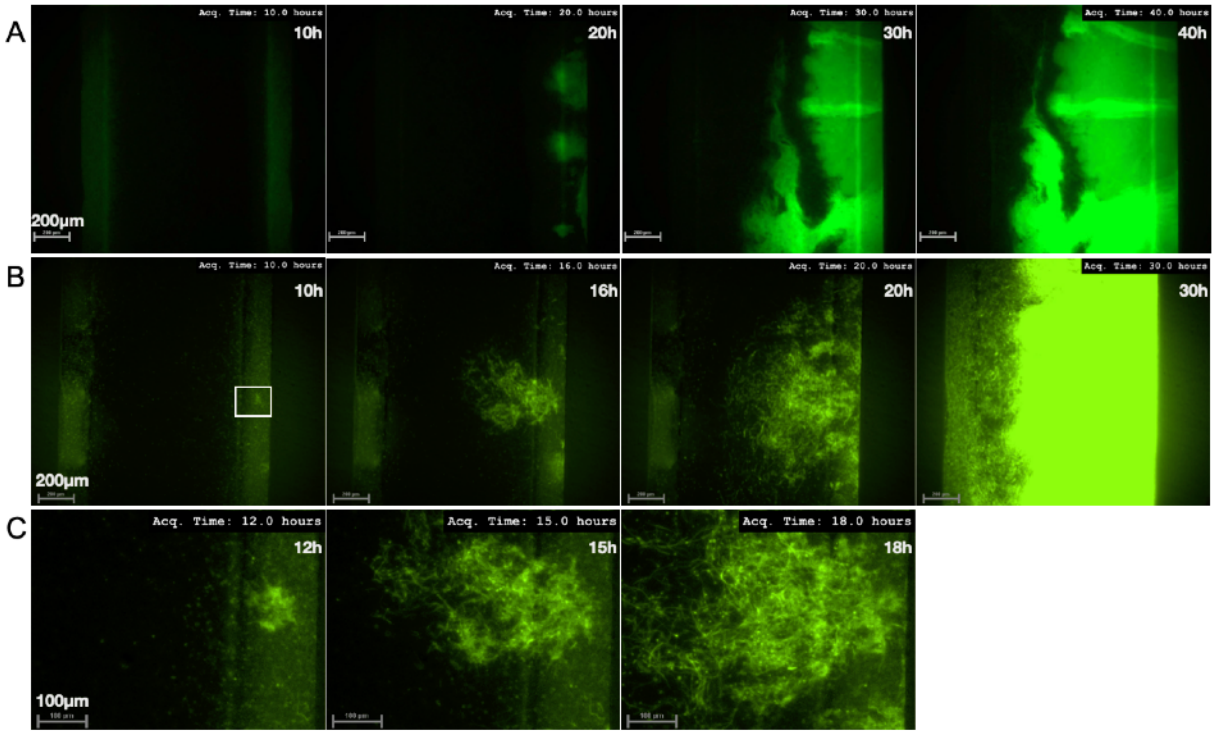

Figure 3. Formation and expansion of resistant E. coli populations in ciprofloxacin gradients. (A-B) *Fluorescent images showing the distribution of bacteria across the observation channel. Maximum ampicillin concentrations (left side) are as follows:* ***(A)*** *3× MIC;* ***(B)*** *6× MIC.* ***(C)*** *Zoom-in images at selected timepoints during the experiment presented in panel B. Images show the growth of a subpopulation and the filamentous morphology of cells.*

I incubated bacteria within the device in the presence of ampicillin gradients for 2-3 days, then I broke the device and collected the cells. I still need to do some replicates, but my results so far suggest that in case of ampicillin gradients there is only a slight increase 2-8× in the measured MIC value. An average of 4× MIC increment was observed within 48 or 72 h.

We performed whole genome sequencing on 3 clones isolated from 3 different experiments. In the sample with the highest resistance level (8× MIC change) we observed changes in the *ampC* (Beta-lactamase) and *ompF* (outer membrane porin) genes. In the other sequenced mutants (with 2× and 4× MIC change) we found mutations in the *rfa* locus (*rfaQ* and *rfaS*) which is

important in the assembly of the outer membrane, and therefore, can have a role in biofilm formation as well.

As a summary, we can conclude that we observed intense biofilm growth emerging from the sublethal ampicillin regions of the chemical gradient. This phenomena is very similar to the one we observed in case of ciprofloxacin gradients. We found increased level of resistance (measured by MIC change) to ampicillin after 2-3 days of incubation time, however this effect is very mild compared to what we found in ciprofloxacin gradients. Some of the altered regions of the genome are the same as in case of ciprofloxacin. Mutations in the *ompF* and the *rfa* locus can be considered as general stress responses in bacteria, since they are not specific for the used antibiotics, but can help to survive different circumstances. Mutations that are part of the general stress response might also happen due to the microfluidic environment itself, but they could provide advantage in the presence of low level antibiotic concentrations. While mutations in *ampC* or *gyrA* protect bacteria against specific antibiotics, ampicillin and ciprofloxacin, respectively. These specific mutations confer higher level of resistance.

1.2 Role of chemotaxis in the observed fast evolution of resistance

A characteristic behaviour of motile bacteria is the chemotactic response to the presence of gradients formed by certain chemicals (e.g. amino acids, signal molecules). It is an interesting question whether antibiotics have any chemoeffector potential at all. “Can bacteria sense the presence of antibiotic gradients?” “Can they move away and escape from high antibiotic dosage area?” “Does a motile bacterial strain have any advantage in antibiotic gradients compared to non-motile or non-chemotatic strains?” These were the questions we wanted to answer during the grant period.

We started to perform two sets of experiments, but we still need to work to answer the above questions.

<u>Evolution experiments: Non-chemotactic mutant *E. coli* strain in antibiotic gradients</u>

I started to repeat the evolution experiments with a non-chemotactic mutant *E. coli* strain (dCheY). My results suggest that motility (and chemotaxis) might contribute to the observed phenomena presented in Section 1.1. Based on my experiments, the mutant strain also tends to form biofilm-like structures in ampicillin and ciprofloxacin gradients at the low antibiotic concentration side of the observation channel. However, the timescale seems to be slower than in the case of the wild type (chemotactic) *E. coli* strain. Based on the couple of experiments I performed, the insensitive population start to grow with an average of 12 hours delay compared to the wild type cells. I collected the cells from the devices (after 3 days of incubation) and measured the MIC values. I didn’t observe more than 2x increase in the MIC.

There could be different reasons for the delayed response of the non-chemotactic mutant population within the microfluidic device. There are different gradients present in our device:

- antibiotic gradient: it has to be investigated if they have any chemoeffector potential.
- nutrient gradients: we have a huge nutrient resource in the reservoirs, however we observed that wild type cells gather on the overlapping regions in the beginning of the experiments. This suggest that the gathering of cells (chemotacting towards the nutrient source), and their enhanced growth at the overlapping regions might help in the formation of biofilm and adaptation to the environment, finally to the evolution of resistance.

To get statistically relevant data on the evolution of the non-chemotactic *E. coli* strain we need to perform more experiments and perform whole genome sequencing.

<u>Chemotaxis experiments in nutrient poor media</u>

We had already studied earlier the effect of homogeneous antibiotic concentrations on the swimming of *E. coli*. And we found that high dosage of different antibiotics cause a decrease in the swimming speed of cells. This is true both for ampicillin and ciprofloxacin. These studies were carried out separated from the microfluidic experiments.

To study the chemoeffector potential of different antibiotics on *E. coli*, we need to perform experiments in media that limits bacterial growth. For these experiments I used a PBS-based chemotaxis buffer media, and BSA to prevent the attachment of cells to the surface. This way, we could detect single cells within the microfluidic gradient generator device. We had already carried out some chemotactic studies in ampicillin gradients before the grant period where we observed a

specific two sided distribution of cells in the observation channel. We wanted to further investigate this phenomena.

As a first step I wanted to see if *E. coli* behaves the same way in gradients formed by ciprofloxacin (Figure 4). I observed a two-sided distribution of the wild type cells, just like in case of ampicillin gradients earlier. Non-chemotactic mutants showed homogeneous distribution over the 8 hour timescale of these experiments.

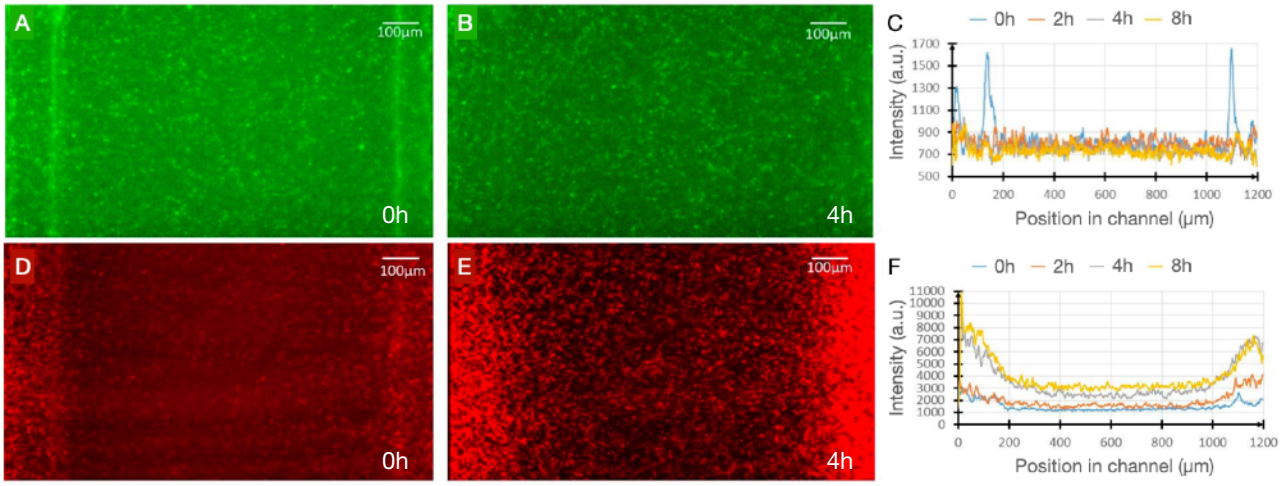

Figure 4. E. coli in ciprofloxacin gradient in nutrient-free media. The maximum antibiotic concentration was 3× MIC (left side) (A-C) *Fluorescence images and corresponding intensity profiles across the observation channel in case of non-chemotactic mutant cells.* ***(D-F)*** *Fluorescence images and corresponding intensity profiles across the observation channel in case of chemotactic wild type cells.*

The observed two-sided distribution must be a result of a different processes that might act separately. Since we see a difference between the examined two strains, chemotaxis might play a role in this phenomena. Also, the deceleration of cells in high concentrations of antibiotics might contribute to it. However, to get a full picture we need further investigations.

We decided to further develop our microfluidic gradient generator setup. Our device in its current form is not suitable to track and measure the swimming speed of motile *E. coli* cells in different parts of the chemical gradient. Therefore, we started to develop a new type of gradient generator device. The development of the hydrogel-PDMS hybrid device was part of the research plan. With this device we would be able to see the cells with high magnification through a thin coverslip even without using fluorescence labels. The details of the device development are summarized in Section 6.1.

To reveal the molecular mechanisms behind the observed partly chemotactic response, in the future we would like to carry out experiments with specific chemoreceptor mutants in the new device. We got the mutants, but I couldn't start the work with them.

2. Emergence of resistance against bacteriophage in structured environment

Beside studying the effect of antibiotic gradients on the emergence of bacterial resistance, I also started a project to reveal whether or not the heterogeneous distribution of bacteriophage causes similar effect on the evolution of resistance in *E.coli* as I observed in case of antibiotic gradients. I did this research in co-operation with the laboratory of prof. Robert H. Austin (Princeton University, NJ, USA). An abstract had been submitted to a special issue in Frontiers in Microbiology ("*Spatial ecology of cells living in micro-structured environments*"), and a manuscript is under preparation based on our results [9].

It is important to better understand what are the mechanisms that can contribute to bacteriophage resistance, because bacteriophage therapy is a promising alternative to antibiotic treatments in case of certain pathogenic microorganisms. However, bacteria can develop resistance *de novo* against phage infections in different ways, which could be a huge challenge during therapies.

There are different mutations that can prevent bacteriophage infection and protect a bacterial population. These mutations usually inhibit the phage adsorption or prevent the injection

of the phage nucleotide. Besides gene mutations, bacteria can use a so called CRISPR system to fight against bacteriophage. The CRISPR-cas system works like an "i*mmune response*", bacteria can detect and destroy DNA from similar viruses during subsequent infection. There are a lot of open questions on how these evolutionary pathways interact and which one is dominant during infections. Besides its medical relevance, it is also important in ecological point of view to study the interaction between bacteria and phage, since they are essential and dominant elements of microbial communities.

Experimental setup

Princeton University has a well-equipped clean room facility, and the Austin Lab has a huge expertise in preparing different microfluidic devices from different materials. For these experiments we used one of their earlier devices, the so called "*Death galaxy*" device with slight modifications. The device was etched into silicon at a 10 μm depth. It contained a network of hexagon chambers (100 μm side length) that were connected through narrow corridors (Figure 5).

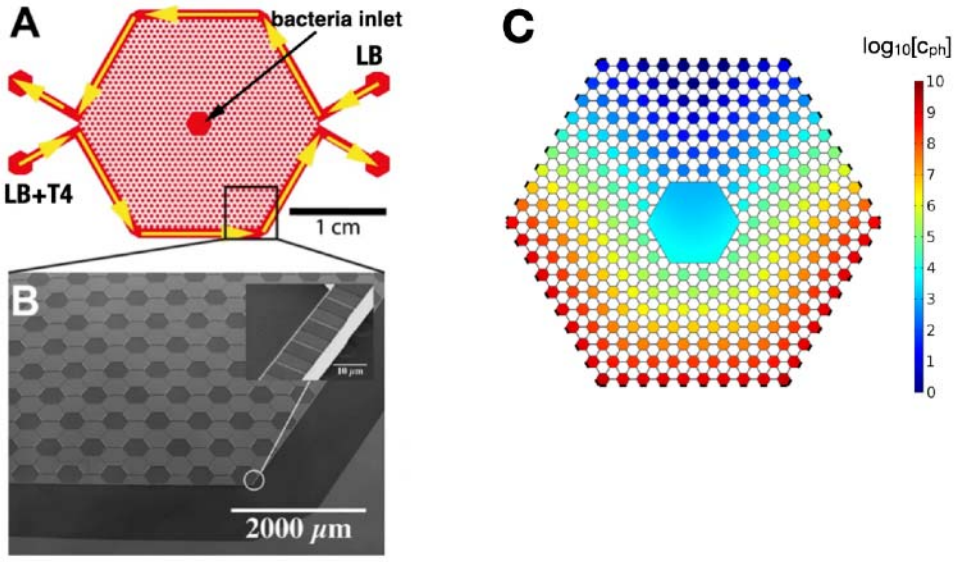

Figure 5. (A) *Schematic drawing of the "death galaxy" device and experimental setup (not-to-scale).* ***(B)*** *Scanning electron microscopy image of the device.* ***(C)*** *3D Comsol simulation of the bacteriophage gradient in the beginning of the experiment when applying 10^9 phage/ml in the bottom side channel and incubated the device for 20 hours before bacteria inoculation.*

Nutrient supply was ensured by two large side channels that encompassed the whole network and were connected by nanoslits (100 nm depth) to the outer chambers. These nanoslits permit the diffusion of nutrients, but prevent bacteria from escaping the chambers. Within this setup, I studied the evolution of resistance in *E. coli* against T4r bacteriophage. By adding T4 particles into the media flowing in one of the side channels, a phage gradient could be formed. Bacteria are injected into the large middle chamber, they can move between patches and explore the environment. Localized metapopulations of bacteria encounter with different number of phage, hence phage titers are distributed across the patches.

3D simulations on the formation of T4r gradient and the distribution of phage over the timescale of the experiments were performed in Comsol Multiphysics software. The concentration of the phage is considered to be constant on the inlets of the nanoslits merging into the T4r containing side channel (bottom side of the device). The diffusion constant of phage ($D_{T4}=10^{-7}$ cm^2/s) was used based on literature data. In the experiments bacteria were inoculated into the middle of the device after 20 hours incubation of the device, during which T4r gradient could form. Figure 5C shows this initial phage distribution when bacteria inoculated into the device. The maximum phage concentration within the device was at least 10^9 particles/ml (bottom side). Initial number of bacteria is 10^4. A fluorescently labelled AB1157 *E. coli* strain was used. Experiments were performed at room temperature.

Fluorescence time-lapse microscopy

Fluorescence time-lapse microscopy was performed for 3-5 days to follow the growth and distribution of bacteria all over the device. We observed that insensitive subpopulations (on the "*phage side*" of the device as well) emerge within 36 hours and spread from biofilm-like pockets. Examples of two such experiments are shown in Figure 6A,B.

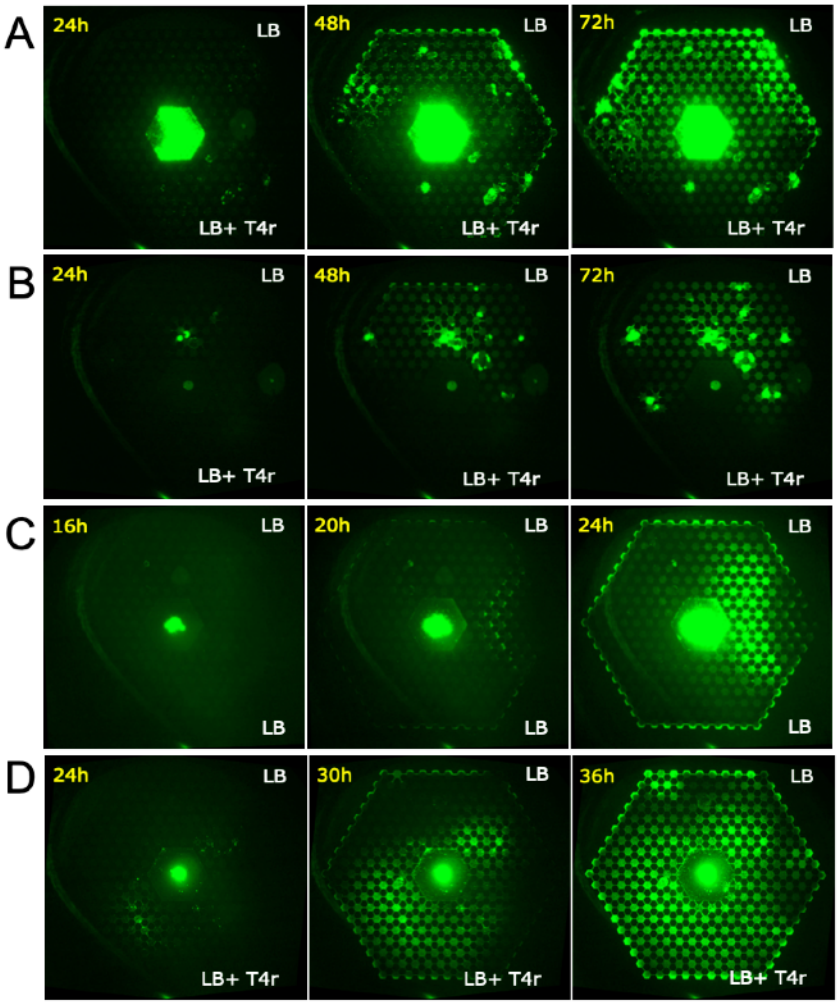

Figure 6. Time-lapse fluorescence images of E. coli in the "Death galaxy" microfluidic device at characteristic timepoints under different conditions. (A-B) *Distribution of E. coli population in the presence of T4r gradient. Biofilm-like cell assemblages can be observed.* ***(C)*** *Growth and distribution of E. coli in the microfluidic device without the presence of phage.* ***(D)*** *The growth and distribution of a mutant strain isolated from a previous evolution experiment in the presence of phage gradient..*

The appearance of the cell assemblages is very interesting. On the "*phage-side*" (bottom part of the device in the images) we do not see much single cells, but mostly these biofilm structures. However, using higher magnification objective, we can detect some motile cells as well. The protective effect of a mature biofilm against phage is well-known, however phage-promoted biofilm formation, what is probably happening in our case, is rare in the literature, little is known about its mechanism.

Control experiment without phage in the device shows rapid distribution and fast growth of bacteria all over the microfluidic device (Figure 6C). Since nutrient supply is coming from the outer side channels, we could also detect the characteristic waves of *E. coli* population consuming the different nutrient sources.

After the experiments the device could be opened and mutants were collected by replica plating the silicon device on agar plates covered by T4r phage. Colonies were selected and further analyzed. I considered the colony resistant if they could perform normal growth in the presence of phage in an amount that otherwise inhibited the growth of the wild type strain. I

selected three clones that we further analyzed by whole-genome sequencing and performed other studies on them. One of the mutants (mut2) has a special mucoid colony morphology.

Repeating the experiments with bacteria isolated from a resistant colony showed almost even distribution within the device in a short time (very similar to the one we observed in the control experiment without phage, Figure 6D).

Whole-genome sequencing

Illumina sequencing was performed on the reference and on the selected three resistant clones. We assembled the entire genomes and compared the genome of the insensitive strains to the genome of the reference (ancestor) strain. We have found mutations at the receptor site of T4 bacteriophage (*ompC*) and in genes (*csg* locus, *rfaP*, *rcsC*) related to biofilm-formation (BF). A list of the most important changes are summarized in Table 1.

Gene	Strain	Related Function	Mutation	Position
ompC_1	P86S1	Outer membrane protein C	Missing Coverage(MC) (8 bp)	201,809
	P86S3	Outer membrane protein C	+T (TAT→TTT)	201,731
csgB	P86S1	Minor curling subunit (BF and Phage Resi)	MC (526 bp)	1807-2333
	P86S2	Minor curling subunit (BF and Phage Resi)	MC (482 bp)	1851- 2333
csgD	P86S1 P86S2	CsgBAC operon transcriptional regulatory protein(Role in BF and fimbriae expression	MC (155 bp)	7607- 7761
rfaP	P86S2 P86S3	Outer membrane lipopolysaccharide core (BF and Phage Resi)	MC (218 bp)	85622- 85839
rcsC	P86S2	Sensor histidine kinase RcsC (BF related)	T→G (CTG→CGG)	196,992

Table 1. Summery of the relevant genes altered upon phage treatment within the "Death galaxy" microfluidic device.

We also analyzed the CRISPR regions of the reference and the mutant strains. We found no changes in the inserts. Which is not so surprising, since none has seen the CRISPR-casE system of *E. coli* in action under normal lab conditions. It is not known what physiological circumstances are needed to activate it. We used a very complex stress landscape (with phage and nutrient gradients) in our studies, but even under these circumstances we did not find new inserts or other changes at the two main CRSIPR regions of *E. Coli*.

We measured the growth properties of the ancestor strain and the mutants under continuous shaking (96 well-plate, 100µl, 37°C) in the presence of phage at the same concentration applied in the microfluidic experiments. Mutants have a normal growth curve even in the presence of high phage titer (Figure 7A).

In the experiments we saw that insensitive populations tend to form biofilm-like structures at certain locations in the microfluidic network, and the observed phage resistance is accompanied by changes in biofilm associated genes. Therefore, it seemed reasonable to check the biofilm forming ability of these mutants compared to the wild type ancestor strain. I performed crystal violet staining to determine the mass of surface-associated biofilm in case of the different strains. The assay was performed in a 96 well-plate, bacteria were incubated for 48 hours at 37°C in static conditions before the staining. Interestingly, I found that the ancestor strain has a larger biofilm mass compared to all the mutants (Figure 7B). However, this does not mean that these strains do not like to form aggregates, but they rather attach to each other than the surface of the plate.

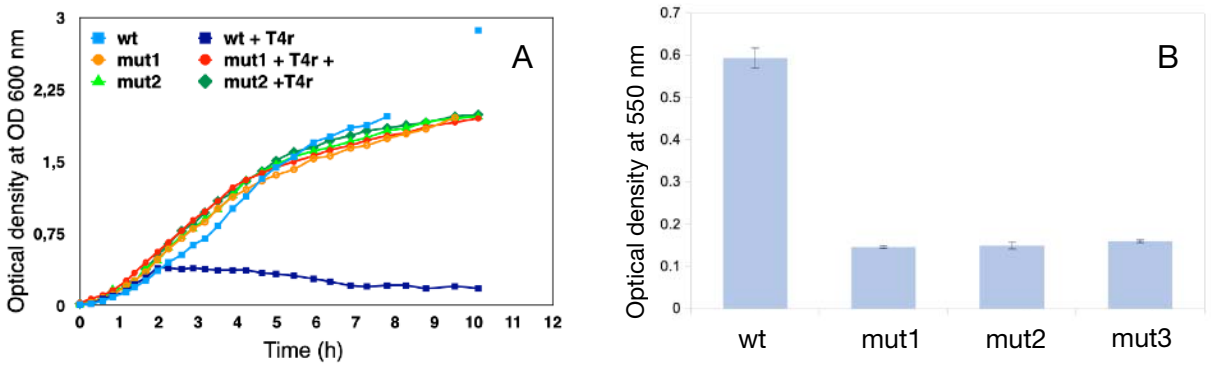

Figure 7. Characterizing the phage resistant mutants. (A) *growth properties of the mutants and the wild type E. Coli strain with and without the presence of T4r phage.* ***(B)*** *The result of crystal violet staining shows the amount of surface associated biofilm formed during 48 h of incubation (37C, static conditions) in 96 well-plate wells by inoculating 100 µl of OD=0.06 bacteria culture.*

Our results strengthen the concept that very specific conditions are needed for the CRSIPR-cas system of *E. coli* to function, and mostly mutations appear in the fight against bacteriophage. Furthermore, our results enhance the importance of phage promoted biofilm formation in the evolution of resistance against bacteriophage.

3.Single-cell level studies on the effect of antibiotics on E. coli

The growth properties and fitness of the wild type *E. coli* strain and the resistant mutants isolated from the evolution experiments are different under different conditions. This is evident form the experiment where we inoculated a mixed culture of the wild type and one of the ciprofloxacin resistant mutant strains into the gradient chip device in the presence of ciprofloxacin gradient (Figure 8). In case of applying 2x MIC maximum concentration of antibiotics, the two strains share the habitat, while in case of a steeper gradient, using 5x MIC ciprofloxacin, the mutant takes over the whole habitat. This suggests that the wild type has a growth advantage in pure LB, whereas the mutant can outcompete the other strain in the presence of ciprofloxacin. Also the biofilm

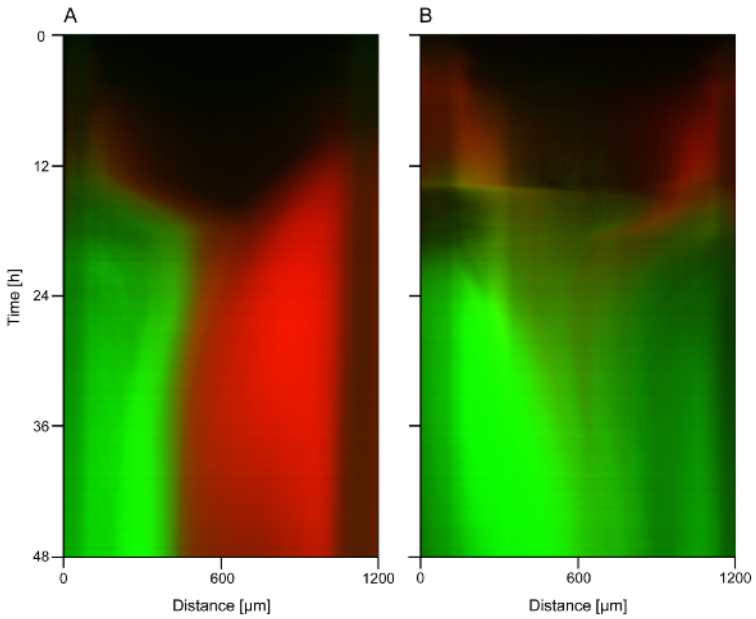

forming ability of these strains are very different.

Figure 8. *Kymographs of fluorescence microscopy images taken during competition experiments of resistant mutants (green color) and the non-resistant ancestor strain (red color) in ciprofloxacin gradients. The applied concentrations are* ***(A)*** *2× MIC on the left side;* ***(B)*** *5× MIC on the left side.*

We would like to further study the isolated mutants from the above-mentioned (Section 1. and 2.) evolution experiments. Also it would be interesting to compare the behaviour of antibiotic and phage resistant strains. Therefore, we started to develop different microfluidic setups in which we can perform single-cell level experiments.

3.1. *E. coli* cultured in a "mother machine" microfluidic device

One of the microfluidic platforms we started to use in our lab is well-known in the literature, it is the so called "*Mother machine*" device. We established this device in our lab and optimized its parameters to study *E. coli* and *P. aeruginosa* bacteria in it. The basic principles of the device is shown in Figure 9. This setup allows us to trap hundreds of cells in individual "growth channels" and monitor their growth in time. It allows us to study a couple of generations together in the 25µm long narrow channels. After a while cells are being pushed out of these narrow side channels and washed away by a continuous flow. Changing the media in the main flow channel is easy and chemicals diffuse fast (in 1s based on simulation data) deep into the growth channels.

In this setup we can measure several parameters, like changes in cell size, cell length, growth rates, generation times. Since the gradient generator microfluidic device in its current form is not suitable to study the morphological changes of bacteria with high magnification, experiments carried out with the "*Mother machine*" device would provide valuable supplementary information to our evolution experiments.

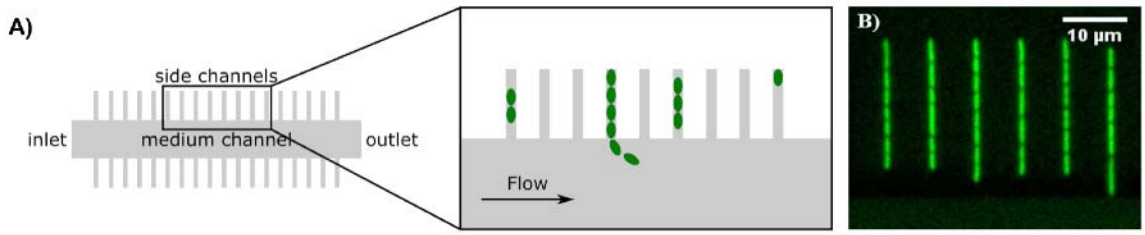

Figure 9. Basic principles of the Mother machine device. (A) *Schematic drawing of the device (not-to-scale).* ***(B)*** *Fluorescently labeled E. coli cells in the growth channels.*

Based on our first experiments, this device is suitable to culture our *E. coli* strain in it (even though this is a motile strain). An example of growing wild type *E. coli* cells in a narrow side channel is shown in Figure 10. The length and the fluorescence intensity of individual cells can be followed in time. The most inner cell stays in the channel during the whole experiment, therefore we analyzed those cells. Divisions can be detected based on the measured length data (it drops down at division events).

Besides, measuring the growth characteristics of different strains under varying conditions, the device is also very promising to study phenotypic heterogeneity in bacteria. We tested the device by flowing LB media supplemented with 3x MIC ciprofloxacin in the main channel. Most of the cells immediately started to elongate. An example of the formation of filamentous cell morphology in a single growth channel over time is presented in Figure 11. Interestingly there is an increased fluorescence intensity for a while, but we do not know the reason for that. When the intensity starts to decrease (after 1200 min) that probably indicates cell death. We can check the viability of the cells within the device by adding propidium-iodide (PI) dye, which only gets into the cell and intercalates into its DNA in case of damaged cell membrane. Not intact cell membrane is an indicator of cell death, bacteria with red fluorescence (stained with PI) are not alive (Figure 11D).

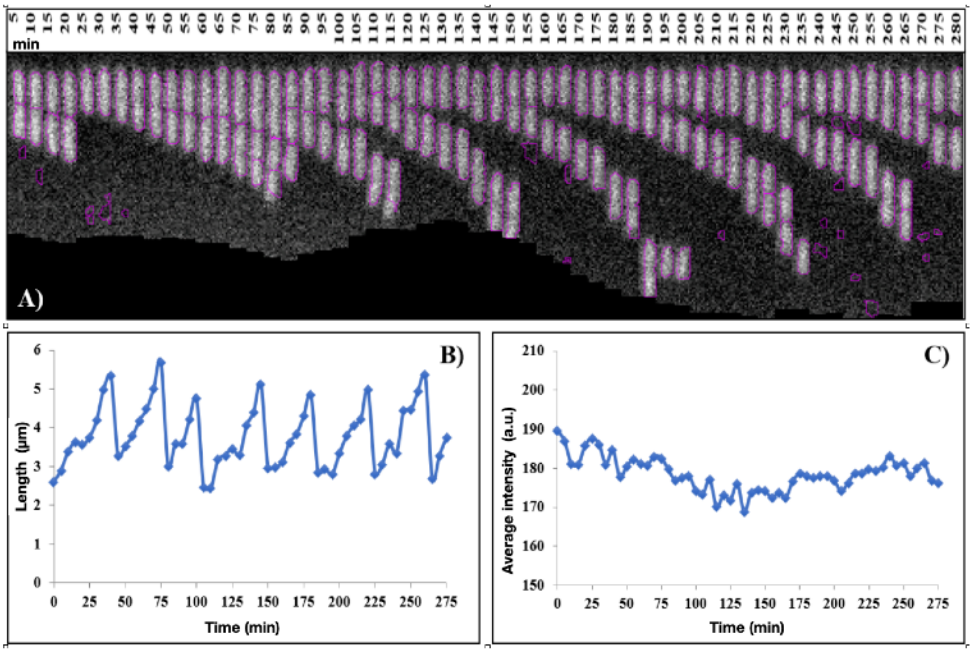

Figure 10. E. coli in the mother machine device. (A) *Kymograph of a single growth channel filled with cells in the beginning of an experiment.* ***(B)*** *Changes in the length of the inner cell within the channel in panel A.* ***(C)*** *Changes in the fluorescence intensity of the inner cell.*

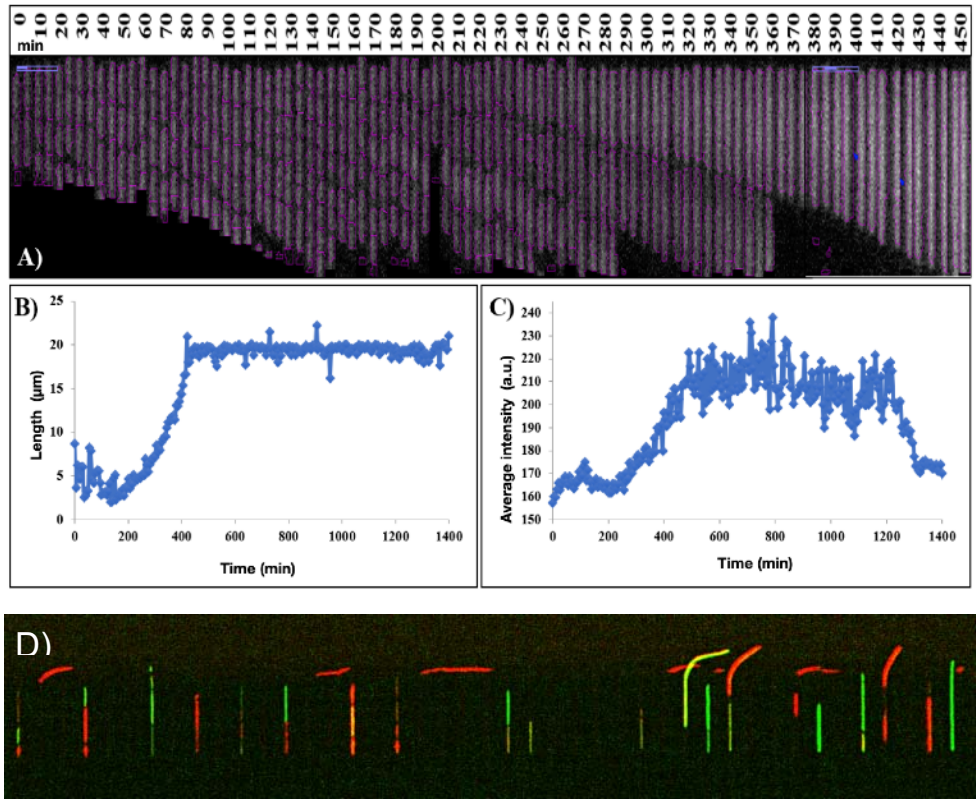

Figure 11. E. coli in the mother machine device under ciprofloxacin treatment. (A) *Kymograph of a single growth channel filled with cells. Filamentous morphology appears upon 3x MIC ciprofloxacin treatment.* ***(B)*** *Changes in the length of the inner cell within the channel in panel A.* ***(C)*** *Changes in the fluorescence intensity of the inner cell.* ***(D)*** *Propidium-iodide staining in the microfluidic device (green cells are alive, red ones are not).*

Occasionally we see cells that do not behave as expected in the presence of ciprofloxacin e.g. the inner cell in Figure 12. only elongates a little bit, but stays in that state during the

timeframe of the experiment. This indicates the phenotypic heterogeneity within the bacteria population.

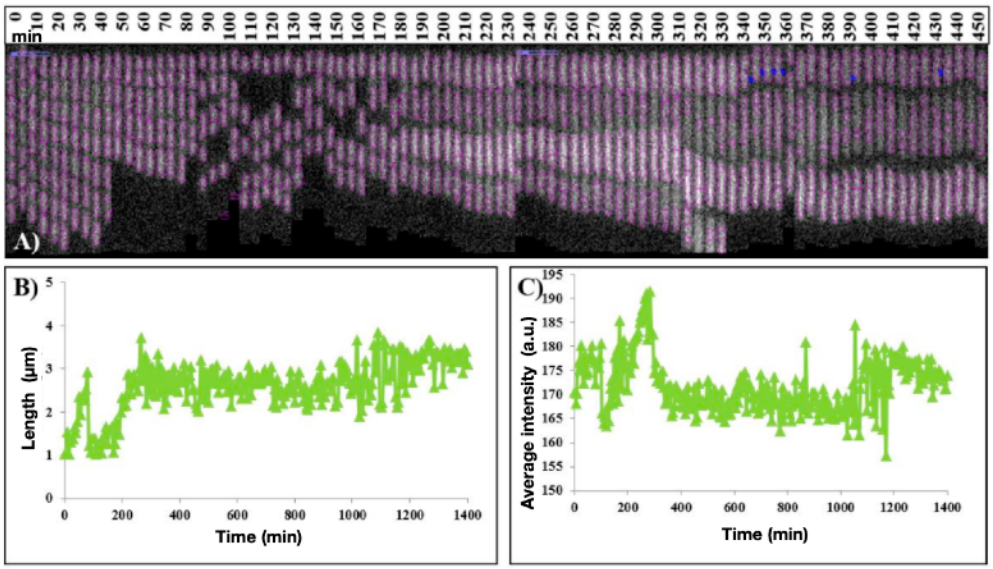

Figure 12. E. coli in the mother machine device under ciprofloxacin treatment. (A) *Kymograph of a single growth channel filled with cells. 3x MIC ciprofloxacin was added into the media.* ***(B)*** *Changes in the length of the inner cell within the channel in panel A.* ***(C)*** *Changes in the fluorescence intensity of the inner cell.*

In the future we would like to use this device and expand our research on studying the heterogeneous response of an *E. coli* population to increasing antibiotic concentrations in time. Temporal gradients of antibiotics might have different effect on bacteria than spatial gradients. Also it would be interesting to see, whether we could observe a "memory" effect when applying antibiotics in a cyclic manner. To perform these experiments we have to modify the current version of this "*Mother machine*" device. We started to develop a similar device but with two inlets. With two inlets and two programmable syringe pumps we can modify the applied antibiotic concentration in very fine steps (almost continuously) and on purpose. Imre Pap, a PhD student co-supervised by me and Péter Galajda is working on this project.

There are studies in the literature that highlight the role of persistent cells in the survivor of a population under stressful conditions. This system might also provide information about the presence of persistent cells in a population.

The single-cell level experiments were not originally planned during the period of the research grant, however we realized the importance of phenotypic heterogeneity in surviving in a dynamically changing environment. Therefore, we expanded our research into this direction.

4. Phenotypic heterogeneity in the qourum sensing system of Pseudomonas aeruginosa

Besides, the emergence of persistent cells, another example of phenotypic heterogeneity occurs during bacterial communication. Quorum sensing (QS) is a well-known bacterial communication system that is widespread among bacteria. QS is used to regulate (and synchronize) gene expression of a population according to cell density. It involves the production and detection of small excreted signal molecules, and controls multiple functions, e.g. bioluminescence, metabolic pathways, motility, biofilm formation, sporulation and virulence. QS has a crucial role in enabling bacteria to orchestrate common actions and form complex communities.

During my grant period I also worked on a project in which we used the above described "*Mother machine*" device to study the dynamics of the QS system in *Pseudomonas aeruginosa* on a single-cell level. *P. Aeruginosa* is a model organism of QS, it has two main QS circuits (LasI-LasR and RhlI-RhlR). In our experiments we used a *lasI*-deficient strain that was not able to produce the signal molecule N-3-oxo-dodecanoyl-L-homoserine lactone, but it could response to its presence. The quorum states of the cells was traced by monitoring the fluorescence emission

of cells due to a reporter plasmid coding for GFP under QS control. The experiment contained three “signal-on” periods, during which cells were continuously exposed to 1μM signal molecule in a nutrient flow, and two “signal-off” periods when we applied nutrient flow without signal molecules. Besides the fluorescence signal, cell size and division were also recorded using time-lapse microscopy. Even cell lineage analysis could be performed. An example of the intensity changes of cells in a single growth channel is presented in Figure 13. together with cell linage data. Altogether 10,766 cells were analyzed during the 64-hour time course of the experiment.

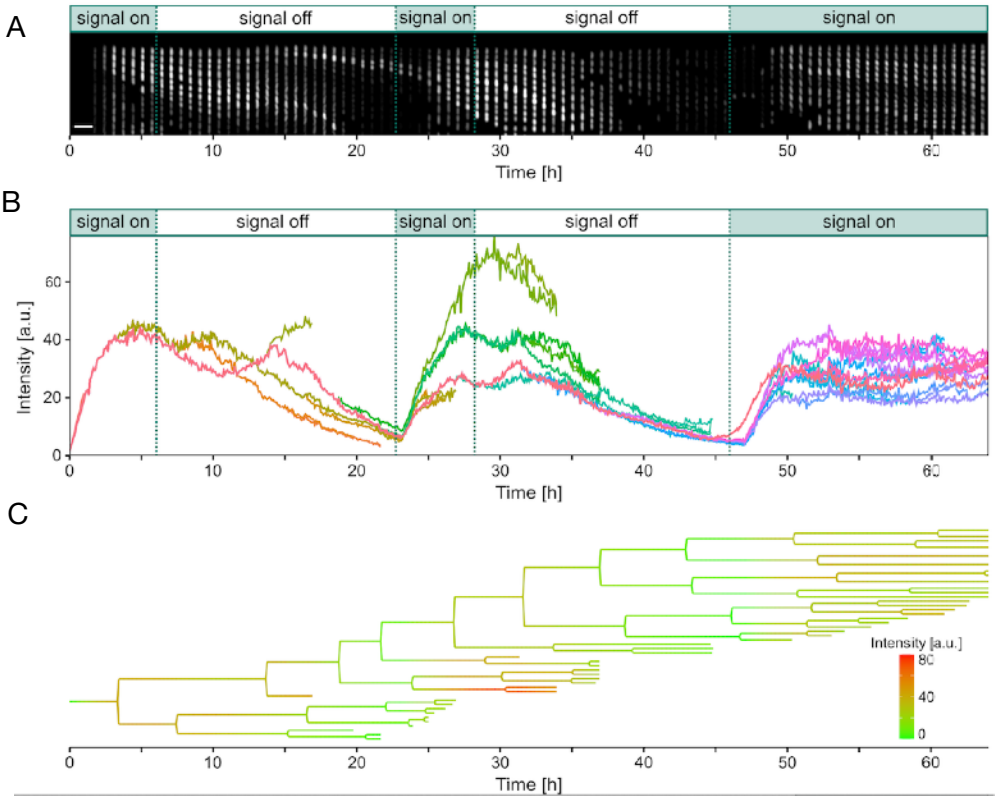

Figure 13. Tracking the quorum sensing behavior of P. aeruginosa cells in a microfluidic mother machine device. ***(A)*** *Kymograph of a single growth channel over the timecourse of the experiment showing the fluorescence intensity changes of cells upon adding/removing the signal molecule. Scale bar is 5 μm.* ***(B)*** *Average fluorescence intensity of the mother cell in panel (A) (most inner cell within a side channel) and its progenies during the experiment. Each color represents another cell that appears upon division. Red curve shows the intensity of the cell with a constantly aging pole (a.k.a the mother cell).* ***(C)*** *Example of a cell lineage tree (for cells shown in panel A) with coloring corresponding to average cellular fluorescence intensity.*

A detailed population-level statistics of the fluorescence intensities is presented in Figure 14. The distributions of fluorescence intensities show unimodal characteristics throughout the experiment. However, the distributions are markedly different at characteristic timepoints, corresponding to signal-on and signal-off scenarios (Figure 14A). Based on these, a threshold intensity can be determined in order to assign QS-on and QS-off states to each cell at all times: cells with intensities over the threshold are said to be in QS-on state, and those below are in QS-off state. A threshold intensity of 12.1 (a.u.) was determined by maximizing the difference between the number of QS-on cells in the signal-on and signal-off periods. Based on this assignment the number (or fraction) of QS-on cells may be followed in time, as shown on Figure 14B. Addition of the signal molecule induces a sharp increase of the QS-on cell fraction. This transition is much steeper than the increase of the fluorescent intensity of cells (Figures 13B and 14C).

We gained a lot of information on the cells throughout the experiment: we measured the cell length, cell length right before division, cell cycle length, elongation rate. Cell length varies a little during the experiment. This suggests that cell size is under tight regulation that is not affected by QS. We determined the average cell cycle length for cells in QS-on and QS-off states during complete cell cycles. We found a higher cell cycle length for QS-on cells (4.8±2.4 h) compared to QS-off cells (3.0±2.1 h).

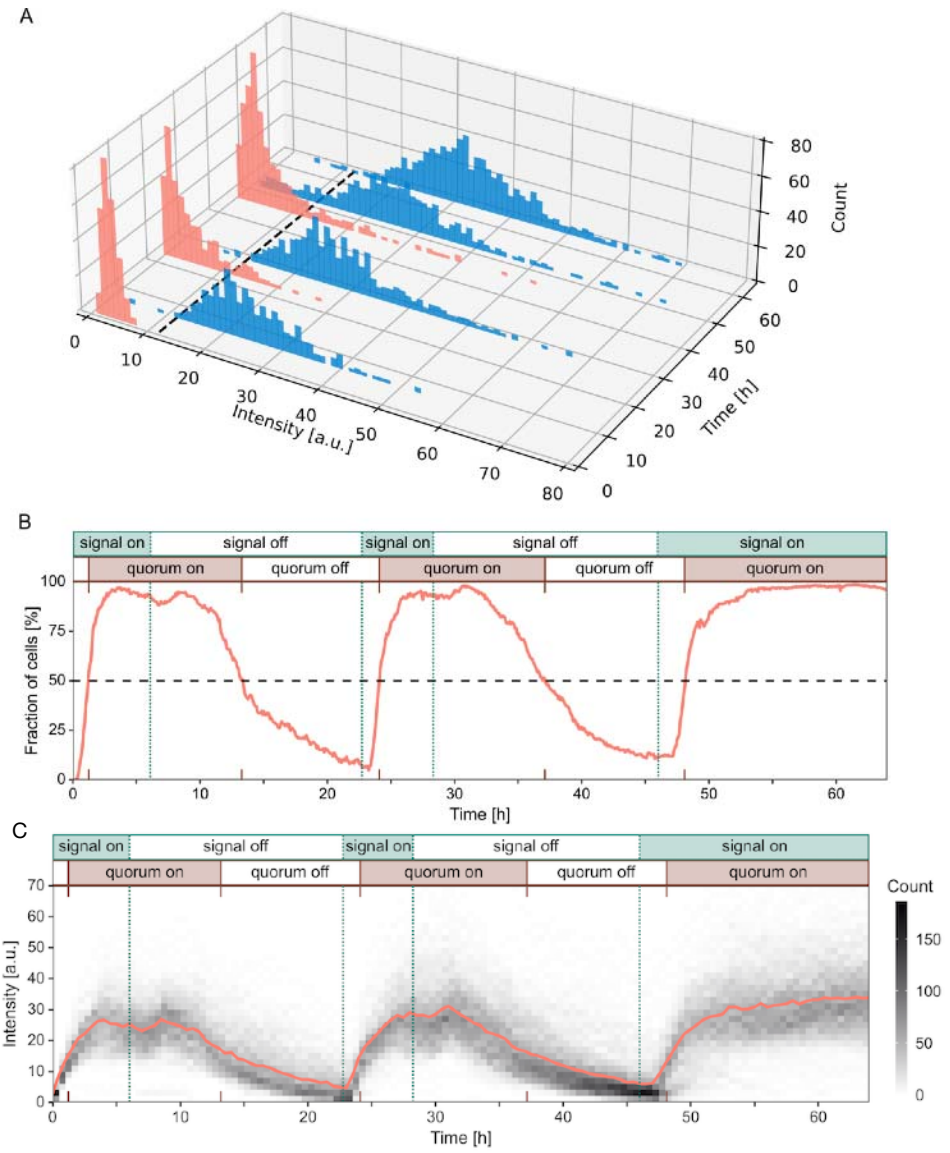

Figure 14. Population-level statistics of the fluorescence intensities of P. aeruginosa cells. (A) *Distribution of the fluorescence intensities of cells within the microfluidic device at characteristic timepoints of the experiment: Red histograms correspond to QS-off periods (t1=0.017h; t2=22.25h; t3=45.5h), and blue ones to QS-on periods (t4=5.58h; t5=27.83h; t6=51h; t7=63.5h).* *Dashed black line indicates the threshold intensity value (12.1 a.u.) determined to distinguish QS-on/off states on a single cell level.* ***(B)*** *The fraction of QS-on cells within the device during the experiment.* ***(C)*** *Fluorescence intensity histograms taken at every 30 minutes. Solid red line shows the population-level average of the fluorescence intensity.*

Due to the construction of the microfluidic mother machine device, cell lineage information can be tracked over the experiments. The cells deepest in the narrow, dead-end growth channels of the device are the so-called mother cells. The pole of the mother cell that falls towards the dead-end of the channel is the old pole, which is inherited from one generation to the next. The other pole is reconstructed in each generation. The aging old pole makes the mother cell special compared to the other cells in the device. Therefore, we compared some of the characteristic cellular parameters between the mother cells and other (non-mother) cells within the device. In terms of the average fluorescence intensity, the difference between the mother cells and all other cells within the device seems to be marginal during the signal-on periods, while in signal-off periods a somewhat faster fall in intensity is observed for the mother cells. A small difference was detected when comparing the average cell length of mother cells to all other cells right before division. We found that the average cell length of the mother cells seems to be somewhat smaller compared to the other cells.

In order to gain some insight into the emergence of cell-to-cell heterogeneity of the fluorescence intensity, we traced the normalized intensity difference between sibling cells during the period of a single cell cycle. Interestingly, we found a linear increase in the relative intensity

difference in time (Figure 15). We treated mother cells and their siblings as a separate group from all other sibling pairs. There is a slight difference between these two groups of cells in terms of the normalized intensity difference. Moreover, there is a higher variability in the mother-sibling group, especially at the late phase of the cell cycle. We also analyzed the intensity difference between siblings in terms of QS state. Here seems to be a slightly higher variability for QS-off cells throughout the whole cell cycle.

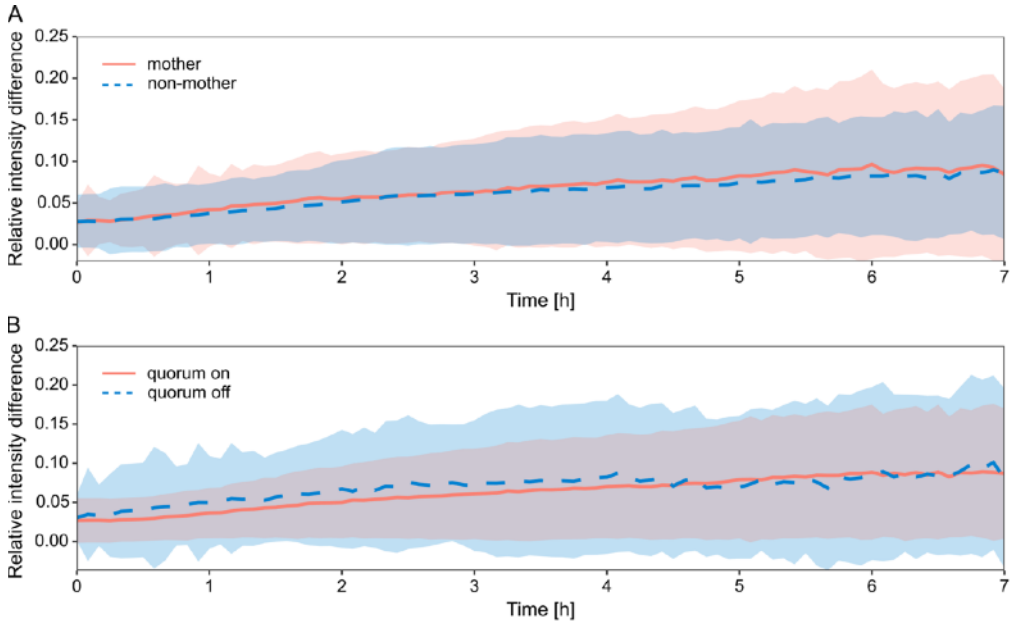

Figure 15. Relative intensity difference between sibling cells during the period of a single cell cycle and its standard deviation. (A) *Intensity difference between mother cells and its closest daughters (solid red line); Intensity difference between all the other (non-mother) sibling cells (dashed blue line).* ***(B)*** *Intensity difference between siblings that stay in QS-on state (solid red line); Intensity difference between siblings that stay in QS-off state (dashed blue line).*

In this section I only presented a brief summary of this research work. Ágnes Ábrahám, our PhD student (whom I co-supervise with Peter Galajda) was highly involved in this project. We have a submitted manuscript in which we also included some other data and a theoretical model for the population level QS response [8].

5. The role of structured habitats in the life of microbial communities

The heterogeneity of the environment affects the life of microbial communities in different ways. Most of the natural habitats (e.g. soil, human body) are structured - “patchy” - both chemically and physically. In our studies we mainly focused on the chemical heterogeneity (antibiotic and nutrient gradients), but physical heterogeneity could also be very important. During the grant period I was involved in a project to study how spatial structure influence the colonization of a habitat by different species and its coexistence. We used a microfluidic device to mimic the complex physico-chemical environment of soil and characterized the patterns of microbial species abundance and distribution in such habitat landscapes.

5.1. *E. coli* metapopulations in patchy landscapes

We studied bacterial metapopulations in patchy habitat landscapes that mimic the spatial structure of soil macroaggregates. The device consists of chambers (100 X 100 x 5 μm) that are connected with narrow corridors of varying width (2-18 μm) (Figure 16). The colonization of the different habitats by *E. coli* was followed in time, the average occupancy of the patches were analyzed.

In the paper we show that Taylor’s law, an empirical law in ecology which asserts that the fluctuations in populations is a power law function of the mean, can be used to analyze the distribution of *E. coli* cells within such landscape. We provide experimental evidence that bacterial

metapopulations in patchy habitat landscapes on microchips follow this law. Furthermore, we found that increased variance of patch-corridor connectivity leads to a qualitative transition in the fluctuation scaling. Our results had been published in Frontiers in Microbiology [3].

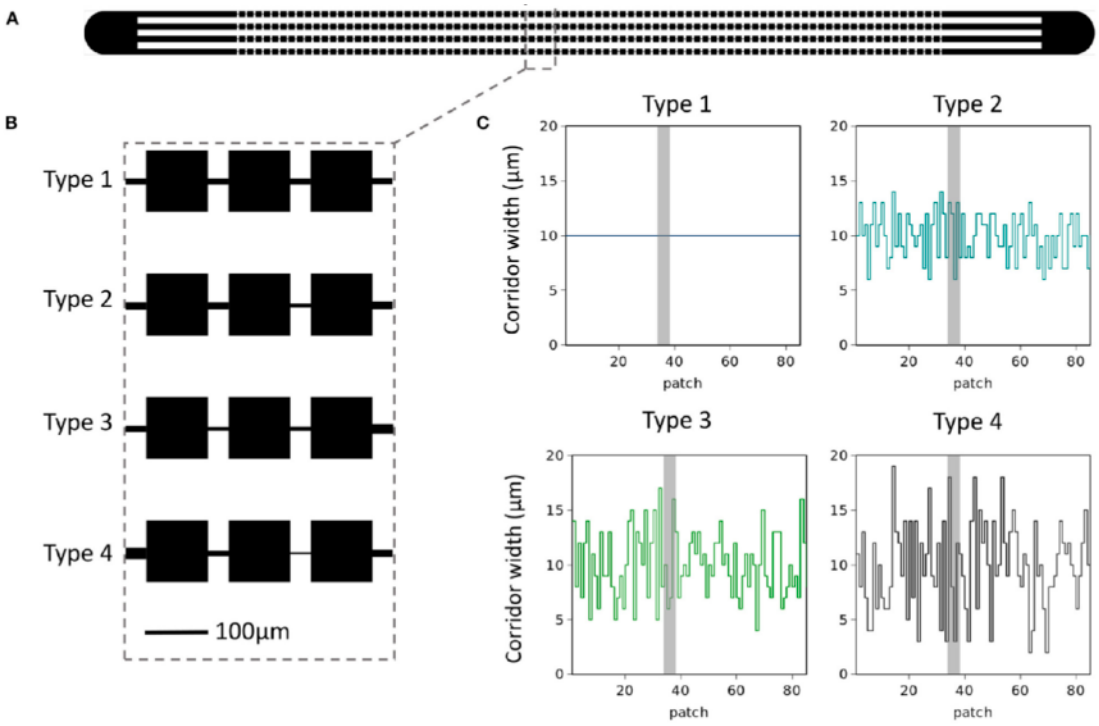

Figure 16. Microfluidics device. (A) *A sketch of the microfluidics device with single inlets on each side leading into four parallel habitat landscapes.* ***(B)*** *Zoom-in view of patch-corridor structure in each of the four parallel landscapes. For type 1 corridor width is kept constant at 10µm. Types 2–4 the average width is also 10 µm with variance around the mean increasing from type 1 to 4 as* $\sigma^2 = 0, 4, 9, 16\ \mu m^2$ *. This can be appreciated in* ***(C)*** *where we show the pattern of corridor widths used for each landscape type. Grey shading indicates location of zoom-in.*

5.2 Competition-colonization strategies in a "patchy" landscape

Using a simplified version of the above mentioned "patchy device", where the corridor width is kept at a constant 10 µm was used to study the competition of *P. aeruginosa* and *E. coli.* These two species represent two different strategies: 1) *P. aeruginosa* is a slow colonizer but a top competitor; 2) *E. coli* is a fast colonizer but a poor competitor. We followed the distribution of cells within the microfluidic landscape by time-lapse fluorescence microscopy and compared these results to batch culture experiments (Figure 17). These kind of experiments are examples for the use of microfluidics in basic ecological problems. In this case we can monitor the ecological succession in a habitat.

Our results suggest that this patchy landscape facilitates the coexistence of these two species. In a batch culture *P. aeruginosa* outcompetes *E. coli*, whereas in a structured habitat *E. coli* finds a way to coexist which is probably due to its fast colonizing strategy compared to *P. aeruginosa* which has a longer lag time before entering into the landscape. We summarized these results in a manuscript together with a theoretical model and this manuscript is under its 2nd revision at *BMC Biology* journal [7].

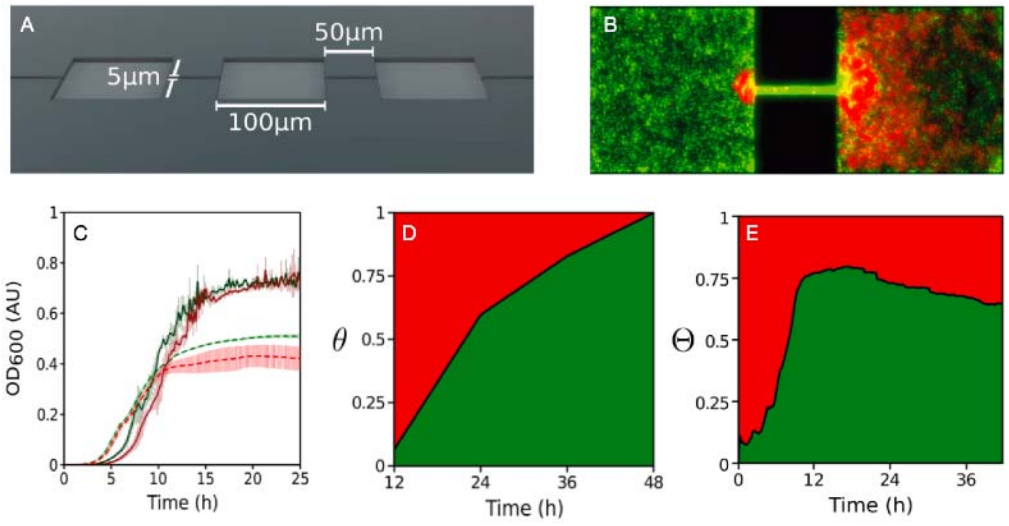

Figure 17. Competition-colonization trade-off in micro-fabricated habitats. (A) *Schematic showing a section of a patchy landscape.* ***(B)*** *Fluorescence microscopy image of the patch-corridor motif depicting E. coli (red) competing against P. aeruginosa (green).* ***(C)*** *Monoculture growth of P. aeruginosa strains (solid lines) and E. coli strains (dashed lines) in well-mixed 96 well-plates.* ***(D)*** *Community dynamics in well-mixed environments represented as P. aeruginosa fractional occupancy, $\theta \equiv \langle N_P /(N_E + N_P)\rangle$; N_P and N_E represent cell counts of P. aeruginosa and E. coli respectively. P. aeruginosa to E. coli initial inoculation ratio 1:1.* ***(E)*** *Metacommunity dynamics in patchy landscapes represented as P. aeruginosa fractional occupancy, $\Theta \equiv \langle \bar{P} /(\bar{E} + \bar{P})\rangle$, calculated as an ensemble average by integrating all 72 landscapes; $\bar{P}$ and $\bar{E}$ represent the spatial average occupancy of P. aeruginosa and E. coli, respectively.*

6. Microfluidic device development

6.1 PDMS-hydrogel hybrid gradient generator device to study bacteria without fluorescence labels

During the grant period we made some efforts to improve the microfluidic gradient generator device. First of all, we wanted to remove the porous membrane that prevents us from detecting unlabeled bacteria in the microchip and it would also allow to take high magnification microscopy images. Our plan was to to use hydrogel walls to separate the chambers (Figure 18A). This would provide better optical qualities for phase-contrast microscopy and single cell detection.

We performed simulations on the gradient formation in such device. The steepness of the gradient between the hydrogel walls could be varied by creating the walls in different thickness (Figure 18B,C). A disadvantage of this device compared to the “sandwich-structured” one, that we used for the experiments so far, is that the formation of the gradient takes more time (Figure 18D,E). It takes about 40 minutes to establish a fully developed gradient.

Poly(ethylene glycol) diacrylate (PEGDA) gels rapidly in room temperature in the presence of a photo-initiator and UV light. We designed and fabricated PDMS devices (with different depth), and managed to polymerize hydrogel structures within these devices. However, we encountered a problem that we could not solve during the grant period. We were not able to create hydrogel structures in the close vicinity of PDMS walls (Figure 19). In the literature we found some hints what problems might occur during the polymerization process, but we were not able to solve this issue.

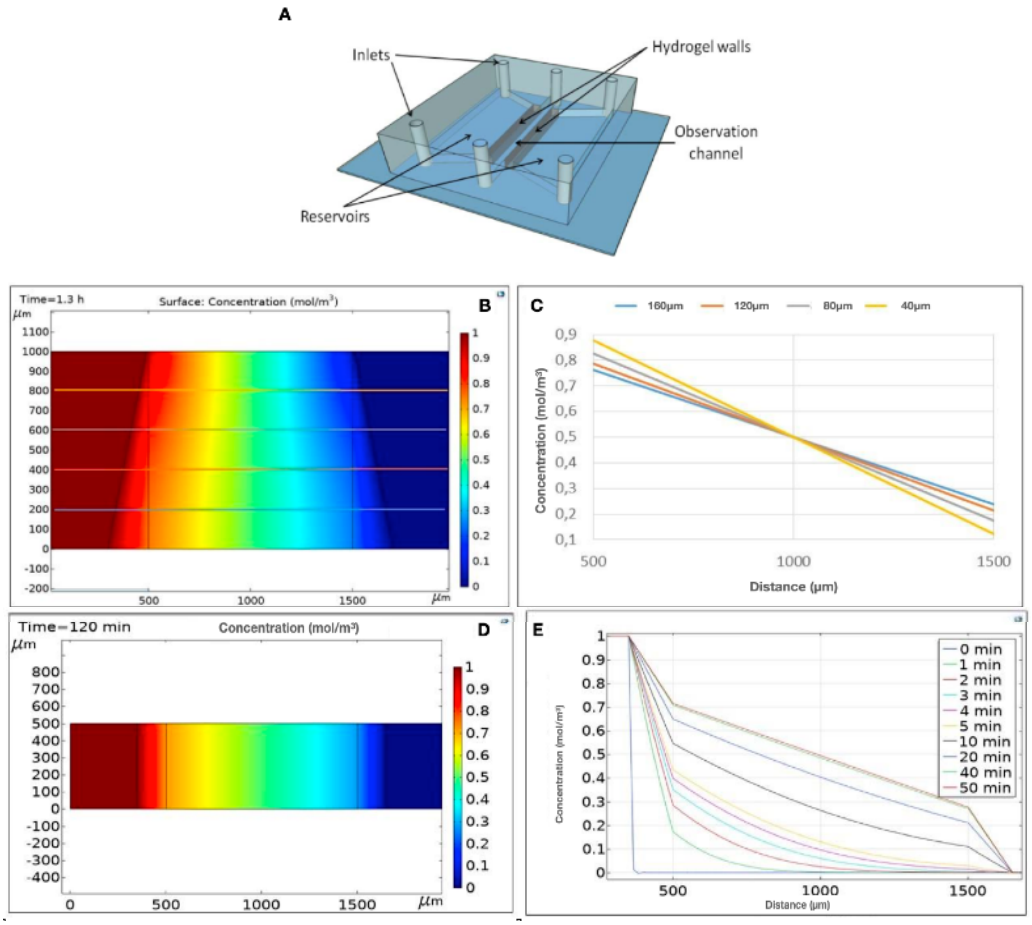

Figure 18. Designing the Hydrogel-PDMS hybrid device. (A) *3D drawing of the device (not-to-scale).* ***(B-C)*** *Fully developed gradients in the device with varying width of hydrogel walls. A narrower wall provides a steeper gradient. (**D-E)** Gradient formation in time in case a 150µm thick hydrogel wall. The concentration falls a lot in the hydrogel wall itself.*

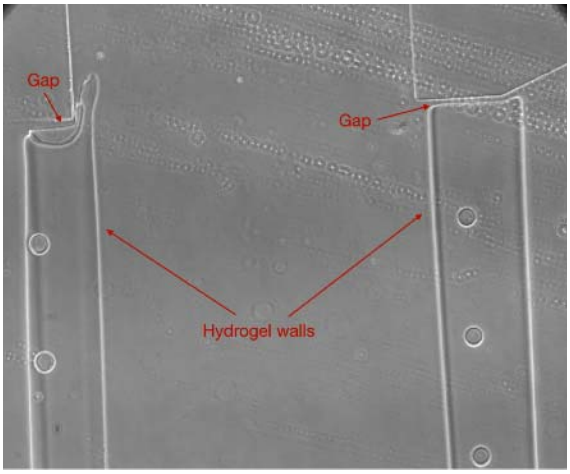

Figure 19. Polymerized hydrogel walls in PDMS device. *Hydrogel structures separate the main channel and reservoirs. Small gaps remained at PDMS walls of the device.*

6.2 Microfluidic device to trap a lot of generations of bacteria in order to study phenotypic heterogeneity: "Baby machine" device

During the grant period we started a project to further develop the previously described "*Mother machine"* device. Our new design would allow to trap single bacteria for a long period, and their characteristic propertiescould be studied by (fluorescence) microscopy. This device would allow

us to follow more generations than it is possible in the "*Mother machine*". Ideally experiments would start from a single trapped cell, and its progenies would be collected over time. We call this device "*Baby machine*". In principle, this way we could better understand how phenotypic heterogeneity emerge within a genetically identical bacterial population. The basic principles of the new design is presented in Figure 20.

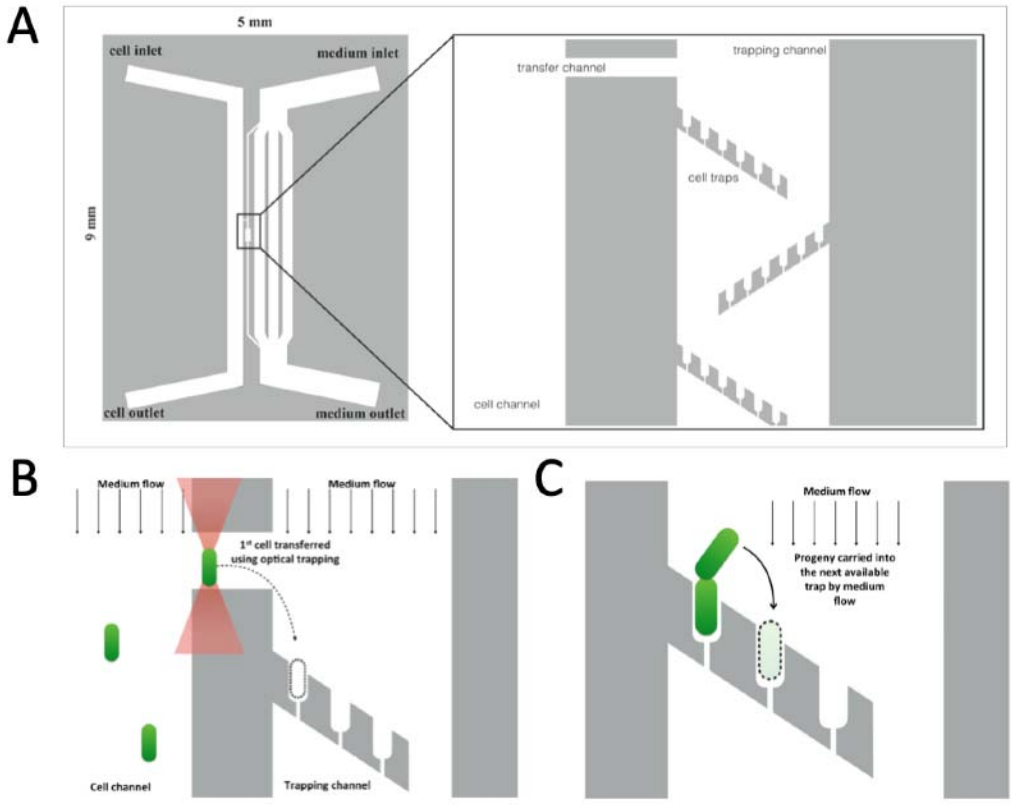

Figure 20. The basic principles of the "Baby machine" device. (A) *Schematic drawing (top view) of the whole device containing the large flow channels (separate for bacteria and for medium flow) and the trapping area.* ***(B)*** *Selected cells could be dragged and placed into the trapping area by the use of an optical tweezer.* ***(C)*** *After positioning a cell in one of the traps, medium flow would keep it there for a long period and its progenies could be collected into the neighbouring cell traps.*

The "Baby Machine" device is a microfluidic channel network. Its main part consists of an array of single cell traps. A single cell is positioned in one of the traps by optical tweezers, then as the cell divides its progenies are collected one by one in the following traps in the array. Time-lapse microscopy allows us to follow the relatedness of trapped bacteria and to measure characteristic cellular parameters. e.g. cell size, morphology, growth rate, gene expression. The 5 mm x 9 mm PDMS device consists of a medium flow channel, a cell channel and a trapping area, which contains bacterial size microfluidic pockets.The height of the device is 30 µm except the trapping part which is comparable to the size of one bacteria.

We performed Comsol simulation on the fluid flow within the trapping area. (Figure 21A) We prepared a version of this device, scanning electron microscopy images show the size of the cell traps (Figure 21B). We have already carried out some test runs. We managed to trap single cells (Figure 21C), however because of some flow issues, in the current setup, some bacteria can get into the medium flow channel which messes up collecting the generations and following them as they fill the traps one-by-one.

The development of this device is in progress, we might have to redesign some parts to solve the mentioned flow issues. However our first results are promising.

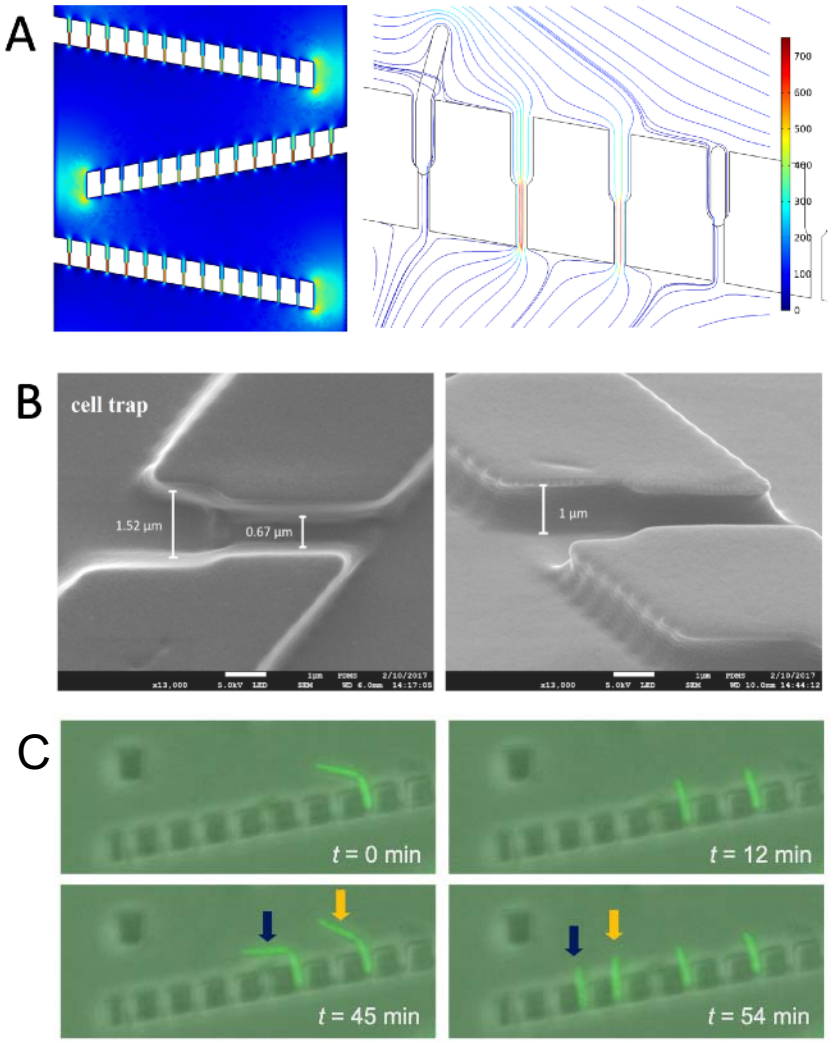

Figure 21. "Baby machine" device. (A) *3D Comsol simulation of the fluid flow in the trapping area Colorbar shows the velocity in µm/s.* ***(B)*** *Scanning electron microscopy images of a single cell trap.* ***(C)*** *Dividing E. coli cells in the trapping area.*

6.3 Microfluidic devices to trap single cells of algae for time-lapse microscopy studies

We designed several types of cell traps for different species and purposes. These devices work based on the principles of microfluidics, mainly on the laminar flow presented in the these systems. We made computer simulations on the flow within these devices to obtain the best layouts for the different microorganisms.

- *Microfluidic platforms to study Chlamydomonas reinhardtii*
  We developed a set of microfluidic devices for morphological and photosynthetic investigations of *C. reinhardtii.* These devices are suitable to trap single cells and perform chlorophyll *a* fluorescence induction measurements on them. The relationship between the morphology and photochemistry of single algae provides valuable information in future biotechnological applications. Heterogeneity in the population could be detected. Results are published in Széles et al. [4].

- *Microfluidic device to study the protoplast formation of Symbiodinium spp.*
  Symbiodiniaceae is a family of dinoflagellate, a group of algae that are endosymbionts of coral polyps. We developed a microfluidic platform which allows the protoplast isolation from individuall trapped *Symbiodinium* cells, by using a precisely adjusted flow of cell wall digestion enymes. Characteristic properties of trapped cells can be monitored during

protoplast formation. The visualization of the intercellular localization of singlet oxygen can also be performed using specific dyes. Our results are summerized in Bashir et al. [6].

SUMMERISING THE MAIN CHALLENGES OF THE RESEARCH PLAN AND THE SUBSEQUENT DIFFERENCES IN THE REALIZED WORK PLAN

During the grant period we focused our interest on the main questions described in the research plan, however, due to some unexpected factors there are some slight differences in some points compared to the original plan.

- It took some time to find the best conditions to perform the evolution experiments. I tested a lot of media, and different antibiotic concentrations before I had the best protocol to follow.
- Our evolution experiments ran longer timescale than expected, and also we sequenced more samples than we planned.
- Because of the above mentioned delays, I mostly focused on the wild-type cells, only a couple of experiments were done with the non-chemotactic mutant strains.
- To move forward with the chemotaxis experiments we started to develop the hydrogel-pdms hybrid device. However, we ran into some unexpected issues during the hydrogel polymerisation. We did not succeed to prepare the hydrogel walls to separate the chambers. Therefore, I could not perform high magnification microscopy to track single cells within the gradient.
- I started a research on the evolution of bacteriophage resistance in a structured environment in cooperation with prof Austin (Princeton University).
- We worked in home office for some months, and had limited access to the lab for a while during the pandemic.

In the past years we recognised the importance of single cell level experiments. Population-level data might obscure the behavior of single cells. Heterogeneity within a bacterial population might have an important role in a stressful environment, (e.g. in the presence of antibiotics). Therefore, we extended our research in developing microfluidic platforms for single-cell level studies. We set up and optimized the "*Mother machine*" device in our lab to monitor the growth of *E. coli* and *P. eruginosa* cells in it. And we also started to design a new device ("*Baby machine*").

This new direction towards trapping and investigating single cells, also brought us new cooperations: We prepared devices to trap *C. Reinhardtii* cells for the group of Szilvia Z. Toth (BRC, Szeged), and we fabricated devices for the group of Imre Vass (BRC, Szeged) to study protoplast formation of *Symbiodinium* spp.

IMPACT AND RELEVANCE OF OUR RESULTS

Microfluidics is an emerging technology that is used more and more in (micro)biology experiments. It offers great tools to create precisely controlled conditions in cellular dimensions which is ideal to explore cell-cell and cell-environment interactions. The available advanced technologies are suitable to create devices for both population and sing-cell level studies. With the help of microfluidics we are able to mimic certain properties of natural habitats during laboratory experiments. Moreover, artificial microfluidic ecosystems can serve as model systems to test ecology theories and principles that apply on higher level in the hierarchy of biological organization. Indeed, we used complex microfluidic devices to study basic ecological questions: habitat colonizastion, succession, competition and evolution.

We wrote a minireview on the potential applications of microfluidics in microbiology and experimental ecology that was published in Frontiers in Microbiology [1]. I also wrote a small paper on this topic in one of the most popular Hungarian science popularization journal, Természet Világa [2].

The ability of bacteria to rapidly evolve efficient mechanisms against antibiotic treatments is a crucial problem for society. Bacteriophage therapy is a promising alternative for antibiotic treatments, however, we might run into the same problem since bacteria can evolve resistance against phage as well. The systematic microfluidic study we performed and our results give

valuable information and shed light on some of the conditions that might contribute to or facilitate this process.

During the grant period we developed a handful of microfluidic platforms that could be used to study different microorganisms. These devices have promising applications in future biotechnology and microbiology studies.

Talks and conferences

I participated and presented my results at several conferences. I gave 4 talks at international conferences and other two at national conferences. I had more than 10 poster presentations. I was invited in giving online courses at the *Women in "Natural Sciences Summer School 2021"* online conference. Besides these scientific forums I also participated in Science popularization events (e.g. Celebration of Hungarian Science; Researcher's night).

Involvement of undergraduate and graduate students

Three PhD students were involved, two of them are working with my joint supervision:
Ágnes Ábrahám (*University of Szeged, co-supervised with Péter Galajda*)
Imre Pap (*University of Szeged, co-supervised with Péter Galajda*)
Miles Wetherington (*P. Catholic University of Chile, supervised by Péter Galajda and Juan E. Keymer*)

Two master and two bachelor students were working in the lab and wrote their diploma work under my joint supervision:
Barbara Dukic (*University of Szeged, MSc in info-bionic engineering, 2017*)
Vanda Zsiros (*University of Szeged, MSc in info-bionic engineering, 2017*)
Rebeka Lukacs (*University of Szeged, BSc in info-bionic engineering, 2020*)
Bence Fürstahl (*University of Szeged, BSc in info-bionic engineering, 2020*)

RELATED PUBLICATIONS

Papers and manuscripts:

1. Nagy K, Abraham A, Keymer JE, Galajda P (2018): Application of Microfluidics in experimental ecology: The importance of being spatial. *Frontiers in Microbiology*. 9. P496

2. Nagy K (2021): Élet egy parányi világban. Baktériumközösségek a természetben és a mikrocsipben. *Természet Világa*. 152. 127-132.

3. Wetherington MT, Nagy K, Der L, Noorlag J, Galajda P, Keymer JE (2022): Variance in landscape connectivity shifts microbial population scaling. *Frontiers in Microbiology*. 13. p831790

4. Széles E, Nagy K, Ábrahám Á, Kovács S, Podmaniczki A, Nagy V, Kovács L, Galajda P, Tóth SZ (2022): Microfluidic Platform designed for morphological and photosynthetic investigations of *Chlamydomonas reinhardtii* on a single-cell level. *Cells*. 11. P285

5. Nagy K, Dukic B, Hodula O, Abraham A, Csakvari E, Der L, Wetherington MT, Noorlag J, Keymer JE, Galajda P (2022): Emergence of resistant *Escherichia coli* mutants in microfluidic on-chip antibiotic gradients. *Frontiers in Microbiology*. 13. p820738

6. Bashir F, Kovács S, Ábrahám Á, Nagy K, Ayaydin F, Valkony-Kelemen I, Ferenc G, Galajda P, Tóth SZ, Sass L, Kós PB, Vass I, Szabó M (2022): Viable protoplast formation of the coral endosymbiont alga Symbiodinium spp. in a Microfluidic Platform. *Lab on a Chip*. *In press* (DOI: 10.1039/d2lc00130f)

7. Wetherington MT, Nagy K, Dér L, Ábrahám Á, Noorlag J, Galajda P, Keymer JE (2022): Ecological succession and competition-colonization trade-off in microbial communities. *under 2nd revision in BMC Biology*

8. Ábrahám Á+, Nagy K+, Dér L, Csákvári E, Pap I, Lukács R, Varga-Zsíros V, Galajda P: Single cell level quorum sensing response of *Pseudomonas aeruginosa* under dynamically changing conditions. (*Submitted manuscript*)

9. *Manuscript in preparation:*
   Nagy K et al.: Emergence of phage resistant bacteria in a microstructured environment (*Sumbitted abstract to a special issue in Frontiers in Microbiology)*

Conference abstract in referred journal:

Ábrahám Á, Nagy K, Csákvári E, Dér L, Galajda P (2019): Exploring phenotypic variability of bacteria using Microfluidic cell traps, *European Biophysics Journal*, 48. Suppl. 1. P-215.